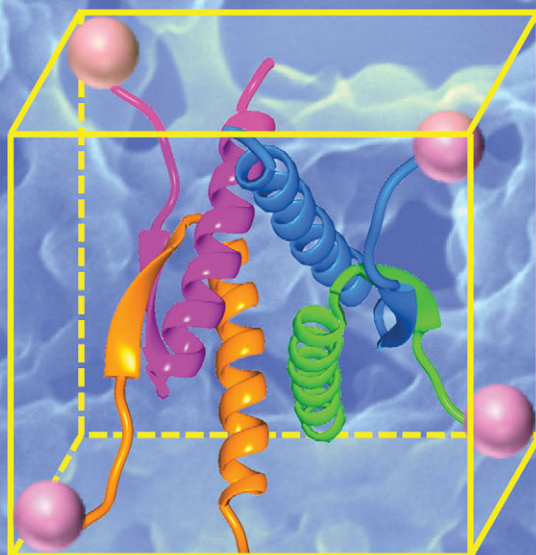


Biomimneralization



Tetramerization

Showcasing research from Prof. Kazuyasu Sakaguchi's Laboratory, Department of Chemistry, Hokkaido University, Sapporo, Japan.

Effects of biomimneralization peptide topology on the structure and catalytic activity of Pd nanomaterials

Catalytically active palladium nanocorals were formed from a designed biomimneralization peptide whose spatial orientation, arrangement and valency were assigned. The topological properties of the peptide were controlled through its conjugation with the p53 tetramerization domain which serves as the 3D control element.

As featured in:



See Kazuyasu Sakaguchi *et al.*,
Chem. Commun., 2014, **50**, 9259.



www.rsc.org/chemcomm

Registered charity number: 207890

Effects of biomineralization peptide topology on the structure and catalytic activity of Pd nanomaterials†

Cite this: *Chem. Commun.*, 2014, 50, 9259

Received 7th June 2014,
Accepted 18th June 2014

DOI: 10.1039/c4cc04350b

www.rsc.org/chemcomm

Jose Isagani B. Janairo,^a Tatsuya Sakaguchi,^a Kenji Hara,^b Atsushi Fukuoka^b and Kazuyasu Sakaguchi^{*a}

Highly branched, coral-like Pd nanostructures were formed using a biomineralization peptide conjugated to an oligomeric peptide that simultaneously controls the spatial orientation, arrangement and valency. The Pd nanocoral showed very high catalytic activity in the reduction of nitrophenol. The results highlight the importance of topological arrangement in nanostructure formation and catalytic activity.

Metallic nanomaterials have gained increased interest in a wide variety of applications, especially in catalysis due to their enhanced properties over bulk materials. The improvement of the catalytic performance of nanomaterials is attributed to their size-dependent surface and quantum confinement effects.¹ Palladium is very important in catalysis since it is involved in a wide spectrum of reactions, ranging from C–C cross coupling to functional group reduction.² Different bottom-up methods can be used to form metal nanostructures, such as the use of stabilizers, templates, and solid supports.^{3,4} Among the different techniques of inorganic nanomaterial synthesis, biomineralization is an emerging, bio-inspired method that utilizes biomineralization peptides (BM Pep) to modulate the nanostructure.⁵ The use of biomineralization peptides offers several advantages over traditional methods of synthesis such as benign conditions, facet binding ability⁶ and self-assembly.⁷ In addition, biomineralization has been successfully applied in the nanostructure formation of relevant metals like Pt, Au, Ag and others.⁸ Recently, efforts to elucidate factors governing biomineralization have been carried out. From these reports, it has been shown that the BM Pep sequence,⁹ the nature of BM Pep binding onto the material surface,¹⁰ BM Pep-metal equivalence¹¹ and buffer type¹² can affect the structure and catalytic activity of nanomaterials formed from biomineralization. It has also been reported that the structure of

the BM Pep acting as a scaffold can also affect the nanostructure and catalytic activity of the biomineralization products.¹³ Therefore, if the spatial orientation, arrangement and valency of the BM Pep can be simultaneously defined, this may have a tremendous impact not only on the resulting nanostructure but also on the catalytic performance of the materials. Thus, we examined the effects of defining the topological properties and valency of the BM Pep on the structure and catalytic activity of Pd nanomaterials.

Our strategy involves the fusion of a BM Pep to a three-dimensional (3D) control peptide. The resulting fusion peptide can simultaneously support the growth of palladium as well as precisely assemble into a well-defined three-dimensional framework, wherein the BM Pep spatial orientation and arrangement are specifically assigned. Porous, hierarchical architectures characterized as coral-like materials were obtained using our designed peptide, which possessed superior catalytic performance in the reduction of nitrophenol isomers. Our results highlight the importance of valency and topological arrangement of the BM Pep in nanostructure formation and catalytic activity.

The control of valency and topological arrangement of the BM Pep was achieved through our designed peptide, Pd4-p53Tet. It is composed of the Pd4 BM Pep conjugated to the N-terminus of the tetramerization domain of the tumor suppressor protein p53 (residues 324–358 of human p53). The Pd4 peptide was identified using a phage display assay and can bind to Pd.¹⁴ The Pd4 BM Pep has been reported to produce dispersed Pd nanoparticles under buffer-free conditions and at peptide: Pd ratios ranging from 1 to 4.¹⁵ The Pd4 BM Pep modulates nanostructure growth through a capping mechanism.¹⁶ The p53 tetramerization domain (p53Tet) on the other hand is one of the five domains of the tumor suppressor p53 protein. The p53Tet is located at the C-terminal region and each monomer within the tetrameric assembly contains a β -strand (residues 326–333), a tight turn (residue 334), and an α -helix (residue 335–356). Two dimers are formed through the formation of a joint antiparallel β -sheet between monomers, and the two primary dimers tetramerize through hydrophobic interactions of the helices in a four-helix bundle.¹⁷ The p53Tet was chosen as the 3D control element

^a Department of Chemistry, Faculty of Science, Hokkaido University, N10 W8, Kita-ku, Sapporo 060-080, Japan. E-mail: kazuyasu@sci.hokudai.ac.jp

^b Catalysis Research Center, Hokkaido University, N21 W10, Kita-ku, Sapporo 001-0021, Japan

† Electronic supplementary information (ESI) available: Detailed experimental procedure, EDX elemental mapping, and catalytic data. See DOI: 10.1039/c4cc04350b

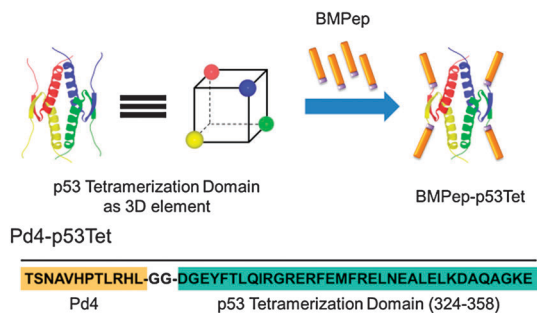


Fig. 1 Design strategy of a fusion biomaterialization peptide with highly defined three dimensional orientation. The fusion peptide is composed of a BMpPep conjugated with a 3D element. The BMpPep used is the Pd4 peptide and the 3D element is the p53 tetramerization domain.

since the positions of the four N-termini in the tetrameric assembly are reminiscent of the vertices of a tetrahedron, which is the simplest 3D object (Fig. 1). The orientation of the N-termini of p53Tet prevents the Pd4 peptides from clashing and interacting with each other while still maintaining a 3D geometry. As a control, the Pd4 BMpPep was similarly conjugated to a variant of p53Tet that cannot oligomerize. This monomeric variant of the p53Tet (p53Mono) consists of three alanine substitutions (L330A, I332A and L344A).¹⁸ The Ala substitutions only alter the oligomerization property of the peptide and do not affect the other properties since there is no change in the number and the type of functional groups of the peptide. Other control peptides include both the native Pd4 and p53Tet sequences.

The respective secondary structures of the synthesized peptides were evaluated by circular dichroism (CD) spectroscopy (Fig. 2).

The CD spectral profiles of Pd4-p53Tet and p53Tet are very similar as expected. This indicates that the Pd4-p53Tet successfully formed tetramers in a similar manner to the native p53Tet and that the Pd4 peptide primarily adopted a randomly coiled structure. The Pd4-p53Mono peptide likewise has a randomly coiled structure. This means that Pd4-p53Mono did not form oligomers (ESI†, Table S2). Biomaterialization was conducted by dissolving the peptides in a HEPES buffered solution (2.5 mM, pH 7.4) to yield a final concentration of 40 μ M of the monomer.

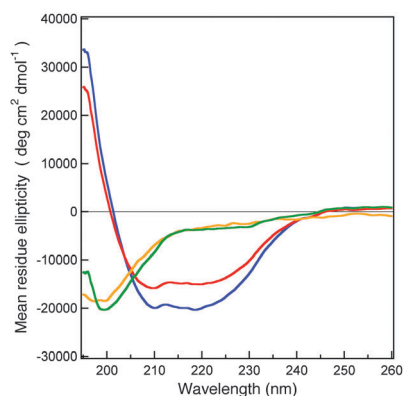


Fig. 2 CD spectra of the synthesized peptides. Red = Pd4-p53Tet; blue = p53Tet; orange = Pd4; and green = Pd4-p53Mono.

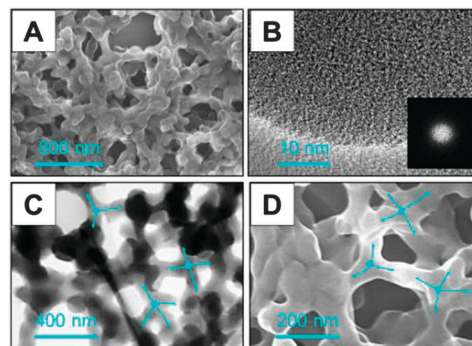


Fig. 3 Representative electron microscopy images of the coral-like Pd structures derived from the Pd4-p53Tet peptide. (A) SE-STEM image showing the porous nature of the Pd structures which emanates from the branched network of filaments. (B) HRTEM image focusing on a section of the filament which shows the absence of lattice lines. The inset is the SAED FFT pattern confirming its amorphous nature. (C and D) STEM images showing the tetrahedral orientation of the filaments at different angles.

A five-fold molar equivalence of K_2PdCl_4 (200 μ M) was added and after 45 minutes, an excess amount of $NaBH_4$ was added. Reduction was allowed to proceed for 90 minutes at room temperature and the resulting materials were purified by centrifugation. The Pd4-p53Tet facilitated the formation of coral-like Pd structures. These nanostructures are porous which arises from a network of branched filaments (Fig. 3A).

This porous characteristic is different from the spherical nanostructures commonly obtained with other biomimetic methods.¹¹ The absence of lattice lines from TEM images in addition to the halo-like selected area electron diffraction patterns taken at multiple areas indicate that the structures are amorphous (Fig. 3B). EDX elemental mapping (ESI† Fig. S1) confirmed that the structures contain Pd. Moreover, the observed carbon and nitrogen signals indicate the incorporation of the peptide template within the Pd nanostructures. The wide distribution of Pd4-p53Tet within the materials possibly explains the amorphous nature of the Pd structures. The Pd4-p53Tet integrates with the material and prevents the Pd atoms from reorganizing into ordered crystalline structures.¹⁹

It was also commonly observed that the Pd4-p53Tet derived nanostructures had several filaments at the pore junction oriented tetrahedrally (Fig. 3C and D). The tetrahedral arrangement stems from the fact that the Pd4 peptide is fused to the spatially-fixed N-termini of the p53Tet and this validates the rationale for the design of the Pd4-p53Tet. This geometric occurrence is a consequence of the controlled oligomerization through the p53Tet.

Comparative structural analysis was performed using the peptide-free, native Pd4 sequence, with p53Tet and Pd4-p53Mono as negative controls (Fig. 4 and Table 1). Small, aggregated particles were formed in the absence of a peptide. The Pd4 BMpPep produced globular aggregates of Pd that resembled solid chains. The p53Tet peptide on the other hand aided the formation of small and dispersed nanoparticles that were irregularly shaped. Finally, a porous thin film which lacked a well-defined and distinct 3D structure was obtained

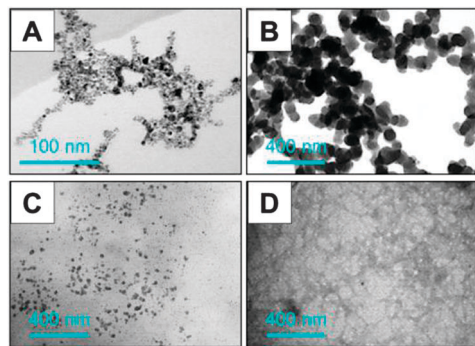


Fig. 4 BF-STEM images of Pd nanostructures prepared in the absence or presence of various peptide sequences. (A) No peptide, (B) Pd4, (C) p53Tet, and (D) Pd4-p53Mono.

from Pd4-p53Mono. The comparative analyses reveal that the coral-like appearance, in addition to the tetrahedral spatial arrangement of the filaments, is exclusively observed for the designed Pd4-p53Tet peptide. The nanocorals were different from the linearly arranged Pd nanoparticles formed using other BMPep in terms of the structure, size and shape.²⁰ Furthermore, the 3D branched morphology of the nanocorals was different from the nanostructures obtained from other reported fusion BMPep. To name a few examples, Au nanoparticle double helices were formed when dodecanoic acid was used as the control element in which the Au BMPep was attached.²¹ Spherical and rod-like morphologies of Ag were formed when different silk protein sequences were conjugated to Ag BMPep.²² When a variant of the cowpea virus was used as the control element for Au BMPep, spherical arrangement of Au nanoparticles resembling the shape of the capsid of the virus was observed.²³ Pd4-p53Tet facilitates nanocoral formation through the combined action of both peptide segments within the Pd4-p53Tet fusion. The nanocoral formation follows a multi-step process. An additional experiment revealed that the 45 minute-incubation period of the peptide with Pd ions prior to reduction is necessary to obtain the 3D porous structure. When the incubation period

was omitted and reduction was immediately done, flat structures with visibly less porosity were formed (ESI† Fig. S2). This suggests that hierarchical nanostructure formation does not proceed spontaneously and involves multiple steps. The pre-reduction incubation period may be necessary in order for the Pd4-p53Tet to properly assemble. Therefore, it is highly plausible that the Pd nanocoral formation with Pd4-p53Tet proceeds through the following stages (ESI† Fig. S3). The Pd4-p53Tet monomers assemble into a tetramer followed by nanostructure growth at the four Pd4 domains that are spatially-fixed, which continues to grow until it is terminated by linking together of similar units.

The catalytic performance of the formed Pd nanostructures was evaluated using the reduction of nitrophenol to aminophenol as the model reaction. NaBH_4 is the reducing reagent wherein a large excess of it in the reaction justifies the use of the integrated rate law ($\ln C_t = -kt + \ln C_0$) for a first order reaction. The rate constant corresponds to the slope of the graph in which $\ln C_t$ was plotted as a function of time. The nanocorals exhibited high catalytic efficiency on the basis of the higher turnover frequency (TOF) for three different substrates compared with those reported in the literature.^{24–26} The Pd4-p53Tet nanocorals possessed much higher activity than the materials obtained from Pd4 and Pd4-p53Mono with respect to the TOF and rate constants (Table 1). The superior catalytic performance of the nanocorals can be attributed to the unique 3D branched structure, defined by a high degree of filament cross-links in different directions. The 3D structure of the materials can influence reactivity.¹¹ On the other hand, the structures obtained from Pd4 and Pd4-p53Mono share the linked morphological feature with the nanocorals but obviously had less 3D character. Comparing the activities of the materials from the Pd4-bearing sequence suggests that increasing the 3D character of the material can lead to the formation of high-performance materials. The nanoparticles obtained under peptide-free conditions showed low activity, most likely due to the aggregation of the particles. In contrast the p53Tet-derived materials showed high catalytic activity. The high activity can be attributed to the small and dispersed nature of the particles, which commonly results in favorable catalytic properties such as

Table 1 Shape, size and catalytic data of the Pd nanomaterials formed from different BMPep for the reduction of nitrophenol isomers

		Turnover frequency (h ⁻¹)		
		(Pseudo-first order rate constants (<i>k</i> , ×10 ⁻³ s ⁻¹))		
	Shape and size	2-Nitrophenol	3-Nitrophenol	4-Nitrophenol
Pd4-p53Tet	Porous, coral-like with a 3D network (Filament thickness = 104 ± 21 nm)	2390 ± 440 (3.10 ± 0.20)	6650 ± 300 (9.37 ± 0.74)	6510 ± 300 (8.63 ± 0.06)
Pd4	Fused, globular particles (Particle diameter = 75.3 ± 9 nm)	600 ± 10 (2.70 ± 0.10)	5640 ± 290 (6.53 ± 0.50)	3150 ± 90 (2.7 ± 0)
Pd4-p53Mono	Network of thin filaments (Filament thickness = 28.5 ± 10 nm)	1580 ± 120 (2.4 ± 0.10)	2740 ± 270 (6.83 ± 0.45)	3020 ± 60 (4.13 ± 0.12)
No peptide	Severely aggregated small particles (Particle diameter = 2.86 ± 0.62 nm)	1660 ± 100 (1.97 ± 0.06)	2930 ± 410 (4.07 ± 0.85)	4170 ± 460 (4.23 ± 0.21)
p53Tet	Irregularly shaped and sized dispersed particles (Particle diameter = 14.4 ± 9 nm)	2500 ± 120 (3.83 ± 0.06)	7100 ± 240 (7.30 ± 0.10)	4990 ± 130 (7.13 ± 0.06)

The average size was determined from a minimum of 100 measurements. Numbers in parentheses correspond to the pseudo-first order rate constants. Numbers above the rate constants are the TOF. Reaction conditions: [substrate] = 50 μM , [Pd] = 0.8 mol%, $[\text{NaBH}_4]$ = 10 mM, 25 $^\circ\text{C}$, triplicate analyses. For a detailed procedure, see the ESI.

alteration of the electronic properties and high surface area, among others.²⁷ Comparing the activities of Pd4-p53Tet and p53Tet shows an interesting observation. The nanocorals were very active despite their larger size. This strongly suggests that the materials with a highly defined 3D structure could give rise to the formation of excellent catalysts. Assigning the topological properties of the BMPep therefore affects not only the nanostructure but the catalytic properties as well. This highlights the importance of specifying the 3D property of the template since the 3D structure of the material depends on it, which influences the catalytic activity. This information expands the knowledge of other known factors that can influence the nanostructure and the catalytic properties of nanocatalysts formed from biomineralization such as the BMPep sequence,⁹ the nature of the BMPep adsorbed onto the nanomaterial surface¹⁰ and metal salt equivalence.¹¹

In summary, we have shown that the precise assignment of the spatial orientation, arrangement and valency of a BMPep can have a significant impact on the resulting nanostructures and their corresponding catalytic performance. The precise topological assignment was achieved through conjugating a BMPep with a 3D control element that can precisely oligomerize into well-defined frameworks. The designed peptide, Pd4-p53Tet, yielded Pd nanocorals with high catalytic activity for the reduction of nitrophenol. The high activity of the nanocorals possibly emanates from the high 3D character of the materials. Our study brings forward the possibility that high-performance materials can be formed by using a 3D-controlled template in order to create materials with well-defined 3D structures. Further studies are still however required to fully elucidate the mechanism behind the formation process; as well as determine the behavior of the material towards the substrates for catalysis. Nonetheless our study expands the existing notion about the factors that affect the nanostructure and catalytic activity of materials formed from biomineralization, such as the BMPep sequence and metal stoichiometry. In addition, our method shows both generality and versatility since other BMPep may be similarly conjugated with the p53Tet thus providing a very flexible method for biomineralization control that can be fine-tuned by choosing a specific BMPep.

This work was supported in part by Grant-in-aid for Scientific Research (B) (No. 24310152) from JSPS (to K.S.), Research Fellowships of the Japan Society for the Promotion of Science for Young

Scientists from JSPS (No. 24-2657) (to T.S.) and a research grant from the Clark Memorial Foundation at Hokkaido University (to J.I.B.J.).

Notes and references

- 1 E. Roudner, *Chem. Soc. Rev.*, 2006, **35**, 583.
- 2 J. Tsuji, *Palladium Reagents and Catalysts*, John Wiley & Sons, UK, 2004.
- 3 A. Fihri, M. Bouhrara, B. Nekoueishahraki, J. M. Basset and V. Polshettiwar, *Chem. Soc. Rev.*, 2011, **40**, 5181.
- 4 D. Astruc, F. Lu and J. R. Aranzas, *Angew. Chem., Int. Ed.*, 2005, **44**, 7852.
- 5 F. Nudelman and N. A. J. M. Sommerdijk, *Angew. Chem., Int. Ed.*, 2012, **51**, 6582.
- 6 C.-Y. Chiu, Y. Li, L. Ruan, X. Ye and C. B. Murray, *Nat. Chem.*, 2011, **3**, 393.
- 7 C. L. Chen and N. L. Rosi, *Angew. Chem., Int. Ed.*, 2010, **49**, 1924.
- 8 M. B. Dickerson, K. H. Sandhage and R. R. Naik, *Chem. Rev.*, 2008, **108**, 4935.
- 9 R. Coppage, J. M. Slocik, M. Sethi, D. B. Pacardo, R. R. Naik and M. R. Knecht, *Angew. Chem., Int. Ed.*, 2010, **49**, 3767.
- 10 Y. Li, Z. Tang, P. N. Prasad, M. R. Knecht and M. T. Swihart, *Nanoscale*, 2014, **6**, 3165.
- 11 R. Bhandari and M. R. Knecht, *ACS Catal.*, 2011, **1**, 89.
- 12 J. I. B. Janairo and K. Sakaguchi, *Chem. Lett.*, 2014, DOI: 10.1246/cl.140405.
- 13 R. Bhandari and M. R. Knecht, *Langmuir*, 2012, **28**, 8110.
- 14 D. B. Pacardo, M. Sethi, S. E. Jones, R. R. Naik and M. R. Knecht, *ACS Nano*, 2009, **3**, 1288.
- 15 R. Coppage, J. M. Slocik, B. D. Briggs, A. I. Frenkel, R. R. Naik and M. R. Knecht, *ACS Nano*, 2012, **6**, 1625.
- 16 R. Coppage, J. M. Slocik, B. D. Briggs, A. I. Frenkel, H. Heinz, R. R. Naik and M. R. Knecht, *J. Am. Chem. Soc.*, 2011, **133**, 12346.
- 17 G. M. Clore, J. Ernst, R. Clubb, J. G. Omichinski, W. M. P. Kennedy, K. Sakaguchi, E. Appella and A. M. Gronenborn, *Nat. Struct. Biol.*, 1995, **2**, 321.
- 18 R. Kamada, T. Nomura, C. W. Anderson and K. Sakaguchi, *J. Biol. Chem.*, 2011, **286**, 252.
- 19 C. H. Lu and F. C. Chang, *ACS Catal.*, 2011, **1**, 481.
- 20 A. Jakhmola, R. Bhandari, D. B. Pacardo and M. R. Knecht, *J. Mater. Chem.*, 2010, **20**, 1522.
- 21 C.-L. Chen, P. Zhang and N. L. Rosi, *J. Am. Chem. Soc.*, 2008, **130**, 13555.
- 22 H. A. Currie, O. Deschaume, R. R. Naik, C. C. Perry and D. L. Kaplan, *Adv. Funct. Mater.*, 2011, **21**, 2889.
- 23 J. M. Slocik, R. R. Naik, M. O. Stone and D. W. Wright, *J. Mater. Chem.*, 2005, **15**, 749.
- 24 J. Li, X. Y. Shi, Y. Bi, J. F. Wei and Z. G. Chen, *ACS Catal.*, 2011, **1**, 657.
- 25 Q. Wang, W. Jia, B. Liu, A. Dong, X. Gong, C. Li, P. Jing, Y. Li, G. Xu and J. Zhang, *J. Mater. Chem. A*, 2013, **1**, 12732.
- 26 X. Wu, C. Lu, W. Zhang, G. Yuan, R. Xiong and X. Zhang, *J. Mater. Chem. A*, 2013, **1**, 8645.
- 27 J. D. Aiken III and R. G. Finke, *J. Mol. Catal. A: Chem.*, 1999, **145**, 1.